



The orthopalladation dinuclear $[\text{Pd}(\text{L}_1)(\mu\text{-OAc})]_2$, $[\text{Pd}(\text{L}_2)(\mu\text{-OAc})]_2$ and mononuclear $[\text{Pd}(\text{L}_3)_2]$ complexes with [N, C, O] or [N, O] containing ligands: Synthesis, spectral characterization, electrochemistry and catalytic properties

Ahmet Kilic^{a,*}, Dilek Kilinc^b, Esref Tas^b, Ismail Yilmaz^c, Mustafa Durgun^a, Ismail Ozdemir^d, Sedat Yasar^d

^a Department of Chemistry, University of Harran, 63190 Sanliurfa, Turkey

^b Department of Chemistry, University of Siirt, 56100 Siirt, Turkey

^c Department of Chemistry, Technical University of Istanbul, 34469 Istanbul, Turkey

^d Department of Chemistry, University of Inonu, 44280 Malatya, Turkey

ARTICLE INFO

Article history:

Received 14 October 2009

Received in revised form 2 December 2009

Accepted 7 December 2009

Available online 6 January 2010

Keywords:

Orthopalladation

Spectroscopy

Catalysis

Suzuki–Miyaura coupling reaction

Hydrogenation

ABSTRACT

Treatment of the salicylaldehyde ligands (L_1H , L_2H , L_3H , L_4H and L_5H) with palladium(II) acetate in absolute ethanol gave the orthopalladation dinuclear $[\text{Pd}(\text{L}_1)(\mu\text{-OAc})]_2$, $[\text{Pd}(\text{L}_2)(\mu\text{-OAc})]_2$ and mononuclear $[\text{Pd}(\text{L}_3)_2]$ with the tetradentate ligands [N, C, O] or [N, O] moiety. The ligands L_1H and L_2H are coordinated through the imine nitrogen and aromatic *ortho* carbon atoms, whereas the ligand L_3H coordinated through the imine nitrogen and phenolic oxygens atoms. The Pd(II) complexes have a square-planar structure and were found to be effective catalysts for the hydrogenation of both nitrobenzene and cyclohexene. These metal complexes were also tested as catalysts in Suzuki–Miyaura coupling of aryl bromide in the presence of K_2CO_3 . The catalytic studies showed that the introduction of different groups on the salicyl ring of the molecules effected the catalytic activity towards hydrogenation of nitrobenzene and cyclohexene in DMF at 25 and 45 °C. The Pd(II) complexes easily prepared from cheap materials could be used as versatile and efficient catalysts for different C–C coupling reactions (Suzuki–Miyaura reactions). The structure of ligands and their complexes was characterized by UV–Vis, FT-IR, ^1H and ^{13}C NMR, elemental analysis, molar conductivity, as well as by electrochemical techniques.

© 2009 Elsevier B.V. All rights reserved.

1. Introduction

Nitrogen donor ligands, such as salicylaldehydes and azines, are prone to undergo cyclometallation reaction with formation of a stable five-membered metallacycle containing a carbon–metal σ bond; many examples of this reaction are known [1–4], and it is important because of its potential use in, e.g., regiospecific organic, organometallic synthesis [5], in catalytic materials [6] and as well as promoting unusual coordination environments [7]. The more common cyclometallated complexes encountered in the literature are the Pd(II) five-membered ring species that have activated aromatic carbon (sp^2) atoms. Analogous compounds containing alkyl carbon (sp^3)–Pd bonds are also known although these are more scarce [8–10]. Among all the examples reported so far those containing square-planar Pd(II) units have attracted special attention due to their potential applications in different areas, including their ability as molecular receptors [11]. Nevertheless, the examples involving Pd(II) blocks containing a σ (Pd–C) bond are not

so common. A few articles focused on the use of bridging bidentate and tridentate salicylaldehyde ligands have been described, but the examples of self-assembly of cyclometallated units are scarce [12]. Also, the reactions of *ortho*-hydroxyazobenzenes with Pd(II) salts to give mononuclear [N, O] [13], [C, N, O] [14] or dinuclear [C, N] [15] cyclometallated complexes have been reported.

The catalytic hydrogenation of benzene and its derivatives generally requires more severe conditions than that of simple olefins [16,17]. Even though a lot of success has been achieved with regard to transition metal complexes in the catalytic hydrogenation of olefins [18–20], there are only few reports on studies involving hydrogenations of arenes using homogeneous metal complex catalysts [21–23]. As a catalyst, palladium is very important in pharmaceutical industry. However, it is expensive and toxic for large-scale applications. It is particularly important to reduce both its loss and presence in a product solution. The ability of transition metal catalysts to add or remove hydrogen from organic substrates by either direct or transfer hydrogenation process is a valuable synthetic tool [24]. Transition metal-catalyzed coupling reaction is one of the most important processes in organic chemistry and has been extensively studied since they represent a powerful and popular method for the formation of carbon–carbon bonds. This

* Corresponding author.

E-mail address: kilica63@harran.edu.tr (A. Kilic).

strategy has been applied to the synthesis of many organic compounds, especially in complex natural products, in supramolecular chemistry and in materials science [25–27]. The importance of biaryl units [26] as components of many kinds of compounds, mainly pharmaceuticals, herbicides and natural products, as well as in the field of engineering materials, such as conducting polymers, molecular wires and liquid crystals, has attracted enormous interest from the chemistry community. Palladium and nickel-catalyzed Suzuki–Miyaura cross-coupling [28–30] is the most important and efficient strategy for the construction of unsymmetrical biaryl compounds. This cross-coupling methodology allows the use of organic solvents and inorganic bases, tolerates many functional groups. It is not affected by steric hindrance of the substrates, and is suitable for industrial processes [31].

In this paper, we describe the synthesis of five new salicylaldimine ligands and their orthopalladated dinuclear $[\text{Pd}(\text{L}_1)(\mu\text{-OAc})_2]$, $[\text{Pd}(\text{L}_2)(\mu\text{-OAc})_2]$ and mononuclear $[\text{Pd}(\text{L}_3)_2]$ metal complexes. We have attempted to prepare Pd(II) metal complexes of ligands L_4H and L_5H to no avail. However, we describe to the best of our knowledge, the synthesis of the first cyclometallated Pd(II) complexes derived from salicylaldimine containing free phenolic-OH tetradentate ligands. In these complexes, the ligands are coordinated through imine nitrogen and aromatic carbon and not through the phenolic OH groups. The compounds have been identified by a combination of ^1H and ^{13}C NMR spectra, FT-IR spectra, UV–Vis spectra, elemental analysis, molar conductivity measurements, and electrochemical techniques. The new orthopalladation dinuclear $[\text{Pd}(\text{L}_1)(\mu\text{-OAc})_2]$, $[\text{Pd}(\text{L}_2)(\mu\text{-OAc})_2]$ and mononuclear $[\text{Pd}(\text{L}_3)_2]$ species exhibited very good catalytic activity towards the hydrogenation of nitrobenzene and cyclohexene. Also, these metal complexes exhibited catalytic activity in the Suzuki–Miyaura coupling of aryl bromide in the presence of K_2CO_3 .

2. Experimental

All reagents and solvents were of reagent-grade quality and obtained from commercial suppliers (Fluka and Merck). Tetra-*n*-butylammonium perchlorate (TBAP, Fluka) was used as received. Elemental analysis was carried out on a LECO CHNS model 932 elemental analyzer. FT-IR spectra were recorded on a Perkin–Elmer Spectrum RXI FT-IR Spectrometer using KBr pellets. The FT-IR spectra of all compounds were carried out in the 4000–400 cm^{-1} range. ^1H NMR spectra were recorded on Bruker-Avance 400 MHz spectrometers. UV–Vis spectra were recorded on a Perkin–Elmer Lambda 25 PC UV–Vis spectrometer. Molar conductivities (Λ_{M}) were recorded on Inolab Terminal 740 WTW Series. The cyclic voltammograms (CV) were carried out using CV measurements with Princeton Applied Research Model 2263 potentiostat controlled by an external PC. A three electrode system (BAS model solid cell stand) was used for CV measurements in CH_2Cl_2 and consisted of a 1.6 mm diameter of glassy carbon electrode as working electrode, a platinum wire counter electrode, and an Ag/AgCl reference electrode. Tetra-*n*-butylammonium perchlorate (TBAP) was used as a supporting electrolyte. The reference electrode was separated from the bulk solution by a fritted-glass bridge filled with the solvent/supporting electrolyte mixture. The ferrocene/ferrocenium couple (Fc/Fc^+) was used as an internal standard but all the potentials in the paper were referenced to the Ag/AgCl reference electrode. The solutions containing ligands and mono- and dinuclear Pd(II) metal complexes were deoxygenated by a stream of high purity nitrogen for at least 5 min. before running the experiment and the solution was protected from air by a blanket of nitrogen during the experiment. GC analyses were performed on a HP 6890N Gas Chromatograph equipped with capillary column (5% biphenyl, 95% dimethylsiloxane) (30 m \times 0.32 mm \times 0.25 μm).

2.1. Synthesis of the salicylaldimine ligands

3,5-Bis(trifluoromethyl)aniline–3,5-dibromosalicylaldimine (L_1H), 3,5-bis(trifluoromethyl)aniline–4-methoxysalicylaldimine (L_2H), 3,5-bis(trifluoromethyl)aniline–5-methoxysalicylaldimine (L_3H), 3,5-bis(trifluoromethyl)aniline–3,5-di-*tert*-butylsalicylaldimine (L_4H) and 2,4-bis(trifluoromethyl)aniline–3,5-dibromosalicylaldimine (L_5H) ligands were synthesized by the reaction of 1.0 mmol (0.23 g) 3,5-bis(trifluoromethyl)aniline in 30 ml absolute ethanol with 1.0 mmol (0.27 g) 3,5-dibromosalicylaldehyde for (L_1H), 1.0 mmol (0.16 g) 4-methoxysalicylaldehyde for (L_2H), 1.0 mmol (0.16 g) 5-methoxysalicylaldehyde for (L_3H), 1.0 mmol (0.24 g) 3,5-di-*tert*-butylsalicylaldehyde for (L_4H) in 35 ml absolute ethanol and 1.0 mmol (0.23 g) 2,4-bis(trifluoromethyl)aniline in 30 ml absolute ethanol with 1.0 mmol (0.27 g) 3,5-dibromosalicylaldehyde in 35 ml absolute ethanol. Also, 3–4 drops of formic acid (HCOOH) were added as catalyst. The mixtures were refluxed for 5–6 h, followed by cooling to room temperature. The resulting crystals were filtered under vacuum. Then, the products were recrystallized from absolute methanol. The products are soluble in common solvents such as EtOH, MeOH, CHCl_3 , DMF and DMSO.

2.1.1. Ligand (L_1H)

Color: orange; m.p.: 138 °C; Yield (%): 68; Anal. Calc. for $\text{C}_{15}\text{H}_7\text{F}_6\text{Br}_2\text{NO}$: C, 36.69; H, 1.44; N, 2.85. Found: C, 37.02; H, 1.72; N, 2.97%. ^1H NMR (CDCl_3 , TMS, δ ppm): 13.93 (s, 1H, –OH, D-exchangeable), 8.62 (s, 1H, $\text{CH}=\text{N}$), 7.87 (s, 1H, Ar–CH), 7.84 (d, 1H, $J = 2.1$ Hz, Ar–CH), 7.73 (s, 2H, Ar–CH), 7.59 (d, 1H, $J = 2.4$ Hz, Ar–CH). ^{13}C NMR (CDCl_3 , TMS, δ ppm): C_1 (163.57), C_2 (157.05), C_3 (148.76), C_4 (139.44), C_5 (134.17), C_6 (133.49), C_7 (133.04), C_8 (121.56), C_9 (121.05), C_{10} (120.12), C_{11} (112.43) and C_{12} (110.97). IR (KBr pellets, cm^{-1}): 3290 $\nu(\text{OH})$, 3104 and 3005 $\nu(\text{Ar-CH})$, 1617 $\nu(\text{C}=\text{N})$, 1277 $\nu(\text{C-O})$. UV–Vis [$\lambda_{\text{max}}/\text{nm}$, (shoulder peak)]: 254, 274, 278, 302, 310, 326*, 363 (in CHCl_3), 249, 297, 319*, 402 (in EtOH) and 260, 284, 309, 351, 446* (in DMSO).

2.1.2. Ligand (L_2H)

Color: yellow; m.p.: 86 °C; Yield (%): 63; Anal. Calc. for $\text{C}_{16}\text{H}_{11}\text{F}_6\text{NO}_2$: C, 52.90; H, 3.05; N, 3.86. Found: C, 52.86; H, 3.06; N, 3.99%. ^1H NMR (CDCl_3 , TMS, δ ppm): 12.93 (s, 1H, –OH, D-exchangeable), 8.58 (s, 1H, $\text{CH}=\text{N}$), 7.77 (s, 1H, Ar–CH), 7.68 (s, 2H, Ar–CH), 7.35 (d, 1H, $J = 8.4$ Hz, Ar–CH), 6.56 (t, 2H, $J = 2.4$ Hz, Ar–CH), 3.88 (s, 3H, O– CH_3). ^{13}C NMR (CDCl_3 , TMS, δ ppm): C_1 (164.34), C_2 (150.34), C_3 (134.36), C_4 (128.55), C_5 (124.93), C_6 (121.41), C_7 (121.32), C_8 (119.57), C_9 (117.70), C_{10} (112.60), C_{11} (107.94), C_{12} (101.06) and C_{13} (55.54). IR (KBr pellets, cm^{-1}): 3274–2385 $\nu(\text{OH}\cdots\text{N})$, 3095 and 3004 $\nu(\text{Ar-CH})$, 2936–2848 $\nu(\text{Aliph-CH})$, 1627 $\nu(\text{C}=\text{N})$, 1279 $\nu(\text{C-O})$. UV–Vis [$\lambda_{\text{max}}/\text{nm}$, (shoulder peak)]: 247, 300*, 344 (in CHCl_3), 245, 302*, 343 (in EtOH) and 273, 304, 355, 376, 409, 451* (in DMSO).

2.1.3. Ligand (L_3H)

Color: orange; m.p.: 89 °C; Yield (%): 71; Anal. Calc. for $\text{C}_{16}\text{H}_{11}\text{F}_6\text{NO}_2$: C, 52.90; H, 3.05; N, 3.86. Found: C, 52.82; H, 2.98; N, 3.93%. ^1H NMR (CDCl_3 , TMS, δ ppm): 12.04 (s, 1H, –OH, D-exchangeable), 8.66 (s, 1H, $\text{CH}=\text{N}$), 7.81 (s, 1H, Ar–CH), 7.71 (s, 2H, Ar–CH), 7.19–6.95 (m, 3H, Ar–CH), 3.84 (s, 3H, O– CH_3). ^{13}C NMR (CDCl_3 , TMS, δ ppm): C_1 (165.42), C_2 (155.71), C_3 (152.58), C_4 (150.21), C_5 (123.17), C_6 (132.72), C_7 (124.85), C_8 (122.20), C_9 (121.55), C_{10} (121.24), C_{11} (119.57), C_{12} (117.62) and C_{13} (55.93). IR (KBr pellets, cm^{-1}): 3295 $\nu(\text{OH})$, 3066 and 3019 $\nu(\text{Ar-CH})$, 2966–2841 $\nu(\text{Aliph-CH})$, 1621 $\nu(\text{C}=\text{N})$, 1280 $\nu(\text{C-O})$. UV–Vis [$\lambda_{\text{max}}/\text{nm}$, (shoulder peak)]: 247, 256, 279, 296, 394* (in CHCl_3), 242, 284, 377 (in EtOH) and 263, 327, 362 (in DMSO).

2.1.4. Ligand (L_4H)

Color: yellow; m.p: 97 °C; Yield (%): 63; Anal. Calc. for $C_{23}H_{25}F_6NO$: C, 62.02; H, 5.66; N, 3.14. Found: C, 61.94; H, 5.73; N, 3.27%. 1H NMR ($CDCl_3$, TMS, δ ppm): 13.05 (s, 1H, –OH, D-exchangeable), 8.73 (s, 1H, $CH=N$), 7.80 (s, 1H, Ar–CH), 7.75 (s, 2H, Ar–CH), 7.57 (d, 1H, $J = 2.4$ Hz, Ar–CH), 7.32 (d, 1H, $J = 2.1$ Hz, Ar–CH), 1.58 (s, 9H, C– CH_3) and 1.38 (s, 9H, C– CH_3). ^{13}C NMR ($CDCl_3$, TMS, δ ppm): C_1 (166.58), C_2 (158.53), C_3 (150.28), C_4 (141.24), C_5 (137.40), C_6 (133.11), C_7 (132.67), C_8 (129.55), C_9 (127.49), C_{10} (124.92), C_{11} (122.18), C_{12} (121.54), C_{13} (120.47), C_{14} (117.69), C_{15} (35.16), C_{16} (34.33), C_{17} (31.52) and C_{18} (29.63). IR (KBr pellets, cm^{-1}): 3432 $\nu(OH)$, 3090 $\nu(Ar-CH)$, 2960–2872 $\nu(Aliph-CH)$, 1607 $\nu(C=N)$, 1280 $\nu(C-O)$. UV–Vis [λ_{max}/nm , (*:shoulder peak)]: 246, 291, 365 (in $CHCl_3$), 231, 287, 363 (in EtOH) and 274, 291, 310, 360* (in DMSO).

2.1.5. Ligand (L_5H)

Color: yellow; m.p: 74 °C; Yield (%): 66; Anal. Calc. for $C_{15}H_7Br_2F_6NO$: C, 36.69; H, 1.44; N, 2.85. Found: C, 36.96; H, 1.52; N, 2.98%. 1H NMR ($CDCl_3$, TMS, δ ppm): 12.95 (s, 1H, –OH, D-exchangeable), 8.57 (s, 1H, $CH=N$) ve 7.96–7.50 (m, 5H, Ar–CH). ^{13}C NMR ($CDCl_3$, TMS, δ ppm): C_1 (163.70), C_2 (157.06), C_3 (150.28), C_4 (146.73), C_5 (141.97), C_6 (139.64), C_7 (134.93), C_8 (134.35), C_9 (127.84), C_{10} (121.10), C_{11} (120.30), C_{12} (116.72), C_{13} (112.50), C_{14} (111.54) and C_{15} (110.88). IR (KBr pellets, cm^{-1}): 3303–2397 $\nu(OH\cdots N)$, 3074 $\nu(Ar-CH)$, 1629 $\nu(C=N)$, 1266 $\nu(C-O)$. UV–Vis [λ_{max}/nm , (*:shoulder peak)]: 242, 255, 270, 356 (in $CHCl_3$), 238, 263, 291, 328, 350 (in EtOH) and 262, 339, 440* (in DMSO).

2.2. Synthesis of the complexes

A solution of palladium(II) acetate (1.0 mmol, 0.23 g) in absolute ethanol (20 ml) was added to a solution of ligands L_1H (2.0 mmol, 0.98 g), L_2H (2.0 mmol, 0.73 g), L_3H (2.0 mmol, 0.73 g), L_4H (2.0 mmol, 0.89 g) and L_5H (2.0 mmol, 0.98 g), in absolute ethanol (50 ml) at 50–60 °C. A distinct color change was observed from the initial colorless solution under a N_2 atmosphere with continuous stirring. After the mixture were evaporated to a volume of 15–20 ml under vacuum by heating 3 h in a water bath. After cooling to room temperature, the solutions were filtered through Celite to remove the all small amount of black palladium formed. Elution with methanol afforded green or brown products after solvent removals, which were recrystallized from methanol to give the desired products as green or brown solids. Then products dried in vacuo at 35 °C. We have attempted to prepare Pd(II) complexes of ligands L_4H and L_5H in different solvents, with no success.

2.2.1. $[Pd(L_1)(\mu-OAc)]_2$

Yield: (56%), color: brown, m.p. = 261 °C. Anal. Calc. for $C_{34}H_{12}Br_4F_{12}N_2O_6Pd_2$ (MW: 1305 g/mol): C, 31.30; H, 0.93; N, 2.15. Found: C, 31.26; H, 1.10; N, 2.34%. $A_M = 21 \Omega^{-1} cm^2 mol^{-1}$, 1H NMR ($CDCl_3$, TMS, δ ppm): 13.40 (s, 2H, –OH, D-exchangeable), 8.63 (s, 2H, $CH=N$), 7.95 (s, 2H, Ar–CH), 7.91 (s, 1H, Ar–CH), 7.86 (d, 1H, $J = 2.4$ Hz, Ar–CH), 7.73 (s, 2H, Ar–CH), 7.68 (s, 1H, Ar–CH), 7.60 (d, 2H, $J = 2.1$ Hz, Ar–CH), 7.34 (d, 1H, $J = 2.4$ Hz, Ar–CH), 1.60 (s, 6H, CH_3COO). ^{13}C NMR ($CDCl_3$, TMS, δ ppm): C_1 (164.12), C_2 (163.59), C_3 (150.19), C_4 (148.78), C_5 (141.58), C_6 (139.48), C_7 (135.88), C_8 (134.17), C_9 (125.04), C_{10} (121.59), C_{11} (120.88), C_{12} (116.61), C_{13} (106.63) and C_{14} (26.93). IR (KBr pellets, ν_{max}/cm^{-1}): 3415 $\nu(OH)$, 3068 $\nu(Ar-H)$, 2917–2848 $\nu(Aliph-H)$, 1727 $\nu(COO)$, 1592 $\nu(C=N)$, 1281 $\nu(C-O)$, 545 $\nu(Pd-N)$. UV–Vis [λ_{max}/nm , (*:shoulder peak)]: 272, 300, 362, 459 (in $CHCl_3$), 255*, 277, 357, 445* (in EtOH) and 260, 302, 354, 434 (in DMSO).

2.2.2. $[Pd(L_2)(\mu-OAc)]_2$

Yield: (52%), color: green, m.p. ≥ 300 °C. Anal. Calc. for $C_{34}H_{12}Br_4F_{12}N_2O_6Pd_2$ (MW: 1169 g/mol): C, 36.98; H, 2.24; N, 2.40. Found: C, 36.48; H, 2.13; N, 2.31%. $A_M = 28 \Omega^{-1} cm^2 mol^{-1}$, 1H NMR ($CDCl_3$, TMS, δ ppm): 8.60 (s, 2H, $CH=N$), 7.89 (s, 1H, Ar–CH), 7.92 (s, 2H, $CH=N$), 7.80 (s, 3H, Ar–CH), 7.63 (s, 2H, Ar–CH), 7.10 (d, 2H, $J = 8.7$ Hz, Ar–CH), 6.24 (dd, 2H, $J = 2.4$ Hz, Ar–CH), 5.56 (d, 2H, $J = 2.4$ Hz, –OH, D-exchangeable), 3.67 (s, 6H, O– CH_3), 1.61 and 1.27 (s, 6H, CH_3COO). ^{13}C NMR ($CDCl_3$, TMS, δ ppm): C_1 (167.19), C_2 (166.79), C_3 (161.95), C_4 (150.43), C_5 (135.94), C_6 (131.84), C_7 (131.39), C_8 (125.86), C_9 (124.97), C_{10} (121.36), C_{11} (113.63), C_{12} (108.28), C_{13} (100.78), C_{14} (55.01) and C_{15} (29.71). IR (KBr pellets, ν_{max}/cm^{-1}): 3410 $\nu(OH)$, 3060 and 3025 $\nu(Ar-H)$, 2925–2853 $\nu(Aliph-H)$, 1738 $\nu(COO)$, 1614 $\nu(C=N)$, 1278 $\nu(C-O)$, 527 $\nu(Pd-N)$. UV–Vis [λ_{max}/nm , (*:shoulder peak)]: 262, 270*, 312, 406* (in $CHCl_3$), 258, 309, 401 (in EtOH) and 269, 309, 399 (in DMSO).

2.2.3. $[Pd(L_3)]_2$

Yield: (62%), color: brown, m.p. ≥ 300 °C. Anal. Calc. for $C_{32}H_{20}F_{12}N_2O_4Pd$ (MW: 830.4 g/mol): C, 46.25; H, 2.43; N, 3.37. Found: C, 46.29; H, 2.64; N, 3.20%. $A_M = 23 \Omega^{-1} cm^2 mol^{-1}$, 1H NMR ($CDCl_3$, TMS, δ ppm): 8.23 (s, 2H, $CH=N$), 7.02 (d, 6H, $J = 3.3$ Hz, Ar–CH), 6.95 (d, 3H, $J = 3.0$ Hz, Ar–CH), 6.92 (d, 3H, $J = 3.3$ Hz, Ar–CH), 3.63 (s, 6H, O– CH_3). IR (KBr pellets, ν_{max}/cm^{-1}): 3060 and 3025 $\nu(Ar-H)$, 2990–2837 $\nu(Aliph-H)$, 1593 $\nu(C=N)$, 1284 $\nu(C-O)$, 544 $\nu(Pd-N)$, 461 $\nu(Pd-O)$. UV–Vis [λ_{max}/nm , (*:shoulder peak)]: 250, 256*, 297, 462* (in $CHCl_3$), 241, 295, 461* (in EtOH) and 261, 296, 449* (in DMSO).

2.3. Hydrogenation procedure

The hydrogenation of nitrobenzene and cyclohexene was carried out in a thermostatic reaction flask (100 ml) at 25 and 45 °C under 760 Torr H_2 with vigorous stirring in dry and deoxygenated 50 ml DMF solution. A catalyst was added into 50 ml DMF and saturated with H_2 gas for 10–15 min. After addition of $NaBH_4$, the mixture was stirred for ca. 5 min. and then nitrobenzene and cyclohexene were transferred into the vessel. Later, the H_2 gas was bubbled again into the flask and the volume of the absorbed H_2 gas was measured periodically. Nitrobenzene and cyclohexene, as identified by means of FT-IR scanning, were completely reduced to aniline and cyclohexane.

2.4. General procedure for the Suzuki–Miyaura coupling reaction

The catalyst (1.0 mmol% of Pd complexes), aryl halides (1.0 mmol), phenyl boronic acid (1.5 mmol), K_2CO_3 (2.0 mmol), diethyleneglycol-di-*n*-butylether as internal standard (30 mg), DMF (3 ml) were all added to a small Schlenk tube and the mixture was heated at 100 °C for 6 h in an oil bath. Then, the mixture was cooled, filtered and concentrated. The purity of the compounds was checked by GC and TLC with NMR. The yields were based on different aryl halides.

3. Results and discussion

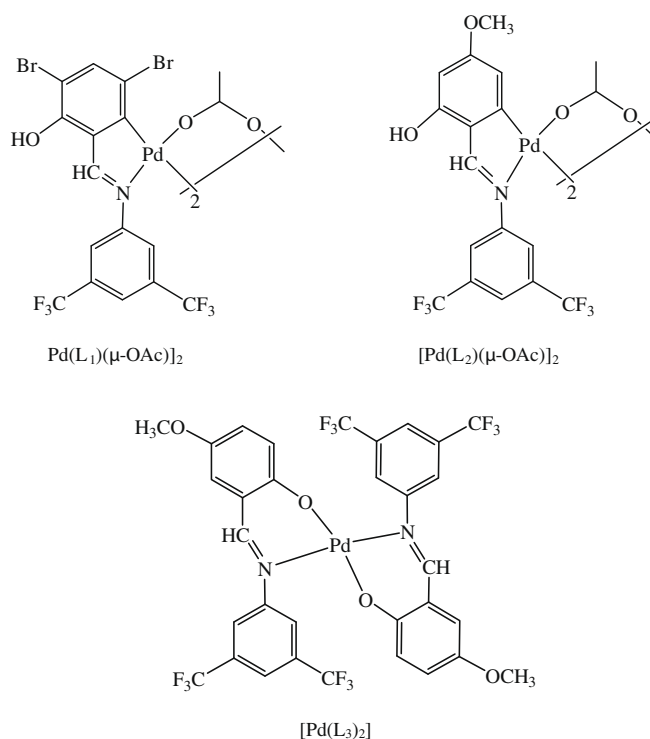
3.1. Synthesis and characterization

The ligands employed provide several coordination approaches as a function of the substitution pattern of the phenyl ring. The ligands L_1H , L_2H and L_3H show available aromatic sp^2 carbon atoms suitable for cyclometallation, as well as OCH_3 and OH substituents liable to carbon–metal and oxygen–metal bond formation. On the other hand, ligands L_4H and L_5H are found to bind to palladium

only through the imine nitrogen and aromatic carbon atoms, not through the phenolic hydroxy groups [15]. Whereas, ligand L₃H coordinates imine nitrogen atom and phenolic hydroxy atom. Hence, in L₁H and L₂H the palladium atom was found to be bonded exclusively through the C₆ atom, with no sign of metallation of the C₂ hydroxy group, resulting in the formation of a five-membered palladated. Whereas, ligand L₃H coordinates *via* the imine nitrogen atom and phenolic hydroxy atom. The cyclopalladation reaction with ligands L₁H and L₂H, which was carried out using palladium acetate in ethanol as described earlier for some other azomethine ligands [32], afforded μ -acetato-bridged dimers [Pd(L₁)(μ -OAc)]₂ and [Pd(L₂)(μ -OAc)]₂. In anhydrous ethanol, the phenolic OH function therefore remains unreactive towards Pd(II), allowing the ortho metallation reaction to take its own course – the Pd–C bond being unreactive [33].

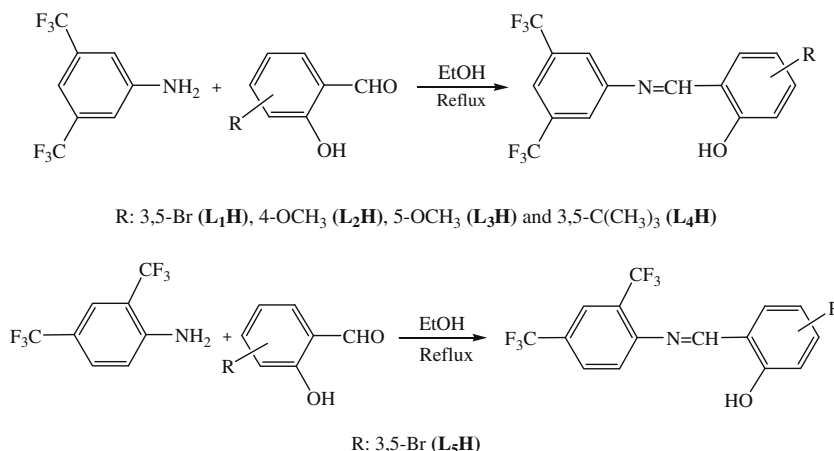
For the convenience of the reader the compounds and proposed structures are shown in Schemes 1 and 2. The compounds described in this paper were characterized by elemental analysis (C, H, N), FT-IR, UV–Vis, ¹H and ¹³C NMR spectroscopy, molar conductivity measurements, and electrochemical techniques. Also, the catalytic activities of the new Pd(II) metal complexes have been investigated. The complexes [Pd(L₁)(μ -OAc)]₂, [Pd(L₂)(μ -OAc)]₂ and [Pd(L₃)₂] were synthesised by the reactions of the ligands with Pd(AcO)₂ in a 1:1 or 1:2 molar ratio in ethanol and shown in (Scheme 2). Magnetic moment measurements of all metal complexes were carried out at 25 °C. The results show that Pd(II) metal complexes are diamagnetic as expected.

The data of the ¹H NMR spectra (in CHCl₃) obtained for ligands and their di- and mononuclear Pd(II) metal complexes are given in the experimental section. The proton resonance is appearing as a broad low intensity singlet at δ = 13.93–12.04 ppm in the spectra ligands (L_{*n*}H) due to the OH...N protons involved in intramolecular D₂O-exchangeable H-bonding. In contrast to expectation, in the ¹H NMR spectra of [Pd(L₁)(μ -OAc)]₂ and [Pd(L₂)(μ -OAc)]₂, a broad singlet peak in a low intensity appeared at δ = 13.40–5.56 ppm due to the presence of the OH protons involved in the dinuclear [Pd(L₁)(μ -OAc)]₂ and [Pd(L₂)(μ -OAc)]₂ (Fig. 1). This result indicates that the (L₁H) and (L₂H) ligands bind palladium ions only through the imine nitrogen and aromatic carbon atoms, not through phenolic hydroxy groups [15,34]. Whereas, this characteristic band are not observed in the ¹H NMR spectra of [Pd(L₃)₂] complex, which indicates that the ligand (L₃H) coordinates to palladium ion through imine nitrogen atom and the deprotonated phenolic hydroxy group. Also, the appearance of acetate methyl groups in the ¹H and ¹³C NMR spectra maybe confirms the formulation of [Pd(L₁)(μ -OAc)]₂ and [Pd(L₂)(μ -OAc)]₂ as typical dinuclear species



Scheme 2. The proposed structure for Pd(II) metal complexes.

with bridging acetate ligands. The chemical shifts of the acetate protons are obtained at 1.60 ppm as singlets for [Pd(L₁)(μ -OAc)]₂ (Fig. 1) and at 1.61 and 1.27 ppm as singlets for [Pd(L₂)(μ -OAc)]₂. Also, the chemical shifts of the acetate methyl carbons are obtained at 26.93 ppm for [Pd(L₁)(μ -OAc)]₂ and at 29.71 ppm for [Pd(L₂)(μ -OAc)]₂. But, these characteristic acetate methyl protons and carbon chemical shifts are not observed in the ¹H and ¹³C NMR spectra of [Pd(L₃)₂] complex. The ¹³C NMR data reveals the different field shifts of the C nuclei relative to the free ligands, while the C=N, C₁ and C₆ resonances reveal different field shifts of the Pd(II) metal complexes, confirming metallation of the phenyl ring [4,35]. In the ¹³C NMR, the imine carbon resonance was found at 157.05 ppm for (L₁H), 150.34 ppm for (L₂H), 155.71 ppm for (L₃H), 158.53 ppm for (L₄H), 157.06 ppm for (L₅H), 150.19 ppm for [Pd(L₁)(μ -OAc)]₂ and 150.43 ppm for [Pd(L₂)(μ -OAc)]₂. The other data of NMR spectra are given in experimental section.



Scheme 1. The synthesis route of proposed ligands.

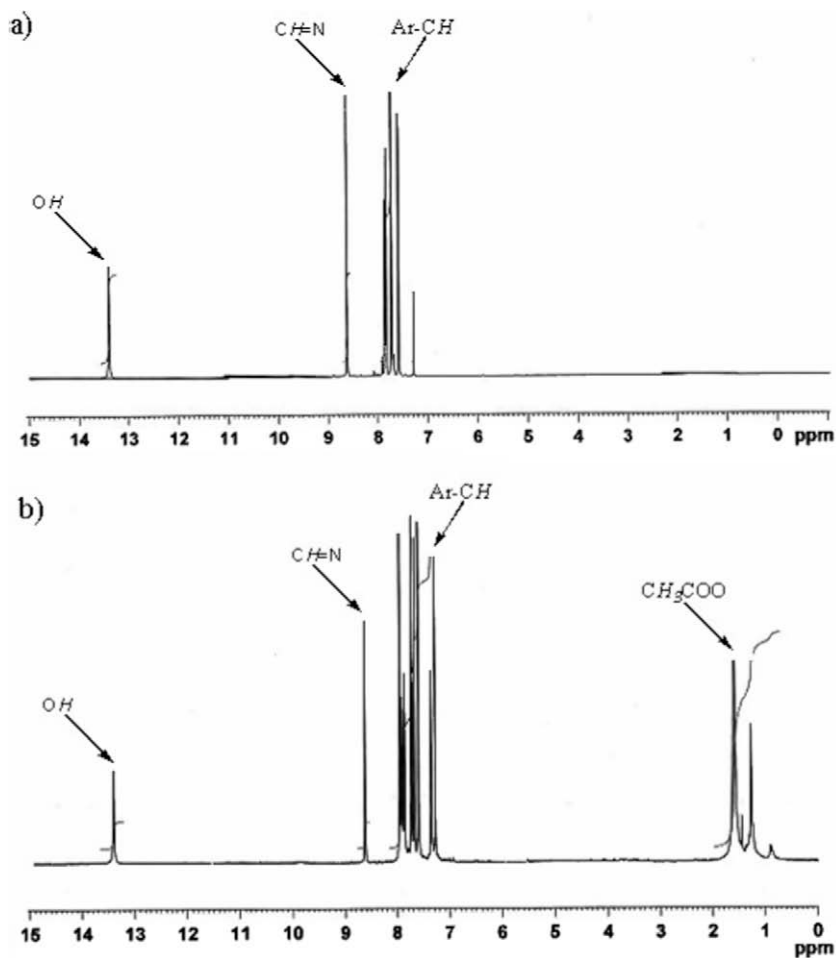


Fig. 1. The ¹H NMR spectrum of L₁H (a) and [Pd(L₁)(μ-OAc)]₂ (b).

The infrared spectra of ligands and their metal complexes have been studied in order to characterize their structures. The main bands in the infrared spectrum for all compounds are given in experimental section. Characteristic absorptions in the spectra FT-IR of ligands and their Pd(II) metal complexes are represented by stretching vibrations of the CH=N group of ligands between 1629–1607 cm⁻¹. The low frequency shift of the CH=N stretch (in between 1614 and 1592 cm⁻¹), in comparison with the free ligands, is consistent with N-coordination of Pd(II) ions to the azomethine ligands [32,36,37]. The coordination of the salicylaldehyde ligands to the Pd(II) center through the azomethine nitrogen atom is expected to reduce the electron density in the azomethine link and lower the ν(C=N) absorption frequency. The spectra FT-IR of ligands are characterized by the appearance of a band at between 3432 and 2385 cm⁻¹ due to the free ν(O-H) or intramolecular ν(O-H...N) groups. In the spectra FT-IR of [Pd(L₁)(μ-OAc)]₂ and [Pd(L₂)(μ-OAc)]₂ complexes, these bands again appear at between 3415 and 3410 cm⁻¹ due to free ν(O-H) group. Whereas, in the spectra of [Pd(L₃)₂] complex, this band is absent. These results show that ligands L₁H and L₂H are found to bind the palladium ions only through the imine nitrogen and aromatic carbon atoms, not through the deprotonation phenolic hydroxy group, whereas, the ligand L₃H binds the Pd(II) ion through imine nitrogen atom and the deprotonation phenolic hydroxy atom. Also, the appearance of ν(COO) bands in the FT-IR spectra at 1738–1727 cm⁻¹ confirms the formulation of [Pd(L₁)(μ-OAc)]₂ and [Pd(L₂)(μ-OAc)]₂ complexes as typical dinuclear species with bridging acetate ligands as obtained previously when using Pd(II)

acetate as the metal salt [38]. Furthermore, additional absorption peaks from the stretching vibrations of the Pd-N, Pd-C and Pd-O bonds appear in the low frequency in all complexes.

Electronic spectra of ligands and Pd(II) metal complexes have been recorded in the 1100–200 nm range and their corresponding data are given in experimental section. The electronic spectra of ligands and their Pd(II) metal complexes in CHCl₃, EtOH and DMSO solutions showed absorption bands at 231–462 nm. In the electronic spectra of the ligands and their Pd(II) complexes, the wide range bands seem to be due to both the π → π* and n → π* of C=N chromophore or charge-transfer transition arising from π electron interactions between the metal and ligand which involves either a metal-to-ligand or ligand-to-metal electron transfer and d-d transitions [39,40]. The absorption bands observed within the range of 231–406 nm are most probably due to the transition of π → π* transitions in the benzene ring or n → π* of imine group or acetate groups corresponding to the ligands and their Pd(II) metal complexes [41]. The electronic spectra of Pd(II) metal complexes show absorption bands at between 406–462 nm are assigned to metal to ligand charge-transfer (MLCT) and ¹A_{1g} → ¹B_{1g} transitions, respectively [42]. In this study, the electronic spectra of all compounds were recorded in the solution state. Thus d-d bands could not be observed [16].

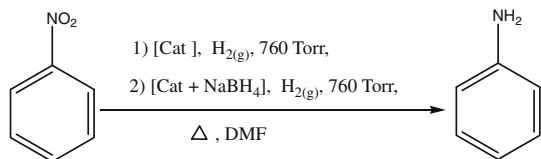
With a view to studying the electrolyte nature of the mono- and dinuclear Pd(II) metal complexes, their molar conductivities were measured in DMF (dimethyl formamide) at 10⁻³ M. The molar conductivities (Λ_M) values of these Pd(II) metal complexes are in the range of 28–21 Ω⁻¹ cm² mol⁻¹ at room temperature, indicating

their almost non-electrolyte nature. Thus, these metal complexes are very poor in molar conductivity (Scheme 2) [43].

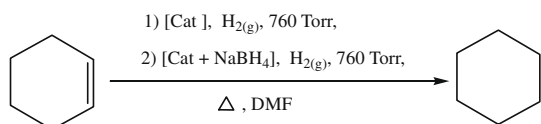
3.2. Catalytic studies

3.2.1. Catalytic reduction of nitrobenzene and cyclohexene by Pd(II) complexes

The catalytic studies showed that the mono- and dinuclear Pd(II) metal complexes exhibited a catalytic activity toward the hydrogenation of nitrobenzene and cyclohexene under H₂ gas (760 Torr) in DMF solution at 25 and 45 °C (Schemes 3 and 4). Nitrobenzene and cyclohexene, as identified by means of FT-IR scanning, were completely reduced to aniline and cyclohexane. Although addition of NaBH₄ to the catalysts solution prior to the introduction of H₂ accelerated their catalytic activity, the hydrogenation did not generally need any preliminary activation (Tables 1 and 2, Figs. 2–7) The conditions, initial rate absorption of H₂, and specific activity for Pd(II) metal complexes are presented in Tables 1 and 2. The course of reduction for some mono- and dinuclear Pd(II) catalysts are shown in Figs. 2–7. The initial rate of H₂ absorption and the specific catalytic activity are approximately identical for all mono- and dinuclear Pd(II) metal complexes. The results indicate that introduction of different groups on in the salicylaldimine ring increases the catalytic activity of all complexes. The electron-donating/withdrawing and other functional groups probably increase the electron density on the Pd atom, which is subjected to electrophilic attack by a nitro group of nitrobenzene and double band of cyclohexene [13,34]. We carried out the same reaction under identical conditions without the catalyst, with organic ligand, with Pd(AcO)₂. In all these three cases no hydrogenation product was detected at the end of the reaction and the FT-IR spectra of compounds have not been changed. These results show that the hydrogenation was catalyzed by the added Pd(II) complex. Finke and co-workers [44,45] reported that the hydrogenation of benzene under vigorous conditions (50–100 °C) using metal complexes proceeds through the formation of M(0) nanoclusters. We have carried out the hydrogenation of nitrobenzene and cyclohexene using the mono- and dinuclear Pd(II) metal complexes at the temperature of 25 and 45 °C. We think that this hydrogenation activity cannot be due to Pd(0), as it is not possible to reduce Pd(II) metal complexes to Pd(0) at 25 and 45 °C. Further in the case of Pd(II) metal complexes, at the end of the reaction there were no particles of palladium metal in the reaction mixture and the addition of mercury, as a selective poison for colloidal/nanoparticle catalysts, to the reaction system does not significantly affect the percentage conversion of nitrobenzene and cyclohexene. From



Scheme 3. Catalytic activity of Pd(II) complexes at 760 Torr of H₂ and 25 and 45 °C for nitrobenzene.



Scheme 4. Catalytic activity of Pd(II) complexes at 760 Torr of H₂ and 25 and 45 °C for cyclohexene.

Table 1

Conditions, initial rate of H₂ absorption, catalytic activity of Pd(II) complexes at 760 Torr of H₂ and 25 and 45 °C for nitrobenzene.

Compounds	[Cat] (10 ⁻⁴ mol/ L)	[Ph-NO ₂] (10 ⁻³ mol/ L)	Initial rate of H ₂ W absorption (mmol/min)	Specific activity mol H ₂ /mol-cat (min)
[Pd(L ₁)(μ-OAc)] ₂	16	2.73	0.04	10.23 (25 °C)
	16		0.06	9.96 (45 °C)
	16		0.05	10.08 (25 °C + NaBH ₄)
	16		0.06	9.91 (45 °C + NaBH ₄)
[Pd(L ₂)(μ-OAc)] ₂	24	2.73	0.05	7.50 (25 °C)
	24		0.06	8.10 (45 °C)
	24		0.03	4.45 (25 °C + NaBH ₄)
	24		0.05	5.80 (45 °C + NaBH ₄)
[Pd(L ₃) ₂]	24	2.73	0.05	7.11 (25 °C)
	28		0.05	6.84 (45 °C)
	24		0.04	4.25 (25 °C + NaBH ₄)
	28		0.04	4.08 (45 °C + NaBH ₄)

Table 2

Conditions, initial rate of H₂ absorption, catalytic activity of Pd(II) complexes at 760 Torr of H₂ and 25 and 45 °C for cyclohexene.

Compounds	[Cat] (10 ⁻⁴ mol/ L)	[Cyclohexene] (10 ⁻³ mol/L)	Initial rate of H ₂ W absorption (mmol/min)	Specific activity mol H ₂ /mol-cat (min)
[Pd(L ₁)(μ-OAc)] ₂	24	3.24	0.01	2.71 (25 °C)
	24		0.01	2.76 (45 °C)
	16		0.02	5.24 (25 °C + NaBH ₄)
	16		0.02	5.61 (45 °C + NaBH ₄)
[Pd(L ₃) ₂]	28	3.24	0.02	2.05 (25 °C)
	24		0.02	2.74 (45 °C)
	28		0.02	2.60 (25 °C + NaBH ₄)
	24		0.02	1.90 (45 °C + NaBH ₄)

these evidences, the hydrogenation of two organic compounds in our system proceeds through a homogeneous mechanism and not through the formation of Pd(0) nanoparticles [16]. From the results shown in Tables 1 and 2, it is evident that the [Pd(L₁)(μ-OAc)]₂ complex is more efficient than the other complexes for the conversion of nitrobenzene to aniline at 25 °C temperature and the [Pd(L₁)(μ-OAc)]₂ complex is more efficient than the other complexes for the conversion of cyclohexene to cyclohexane at 45 °C temperature and in the presence of NaBH₄. The catalytic activities are maybe correlated with the size of the Pd(II) metal complexes, location of substituent, the temperature of reactions and the absence/presence of NaBH₄.

3.2.2. Suzuki–Miyaura coupling reaction by Pd(II) complexes

The nature of the initial precatalyst, solvent and base is crucial for the success of the Suzuki–Miyaura coupling reaction. The reaction condition screen demonstrated that the catalytic activity of Pd(II) metal complexes in Suzuki–Miyaura coupling reaction is highly solvent and base dependent (Scheme 5). Among palladium-catalyzed cross-coupling processes, the Suzuki reaction of aryl/vinyl halides with boronic acid is one of the most efficient methods for C–C bond formation. We did the optimization experiments and we found that when the reaction is carried out using K₂CO₃ in mixture of DMF and water at 100 °C (6 h) the best result

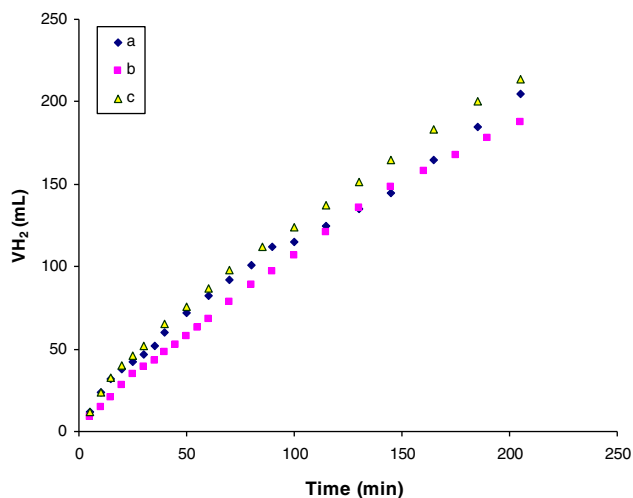


Fig. 2. Hydrogenation of nitrobenzene as catalysts Pd(II) complexes at 25 °C in DMF solution. (a = $[\text{Pd}(\text{L}_1)(\mu\text{-OAc})]_2$, b = $[\text{Pd}(\text{L}_2)(\mu\text{-OAc})]_2$, c = $[\text{Pd}(\text{L}_3)_2]$).

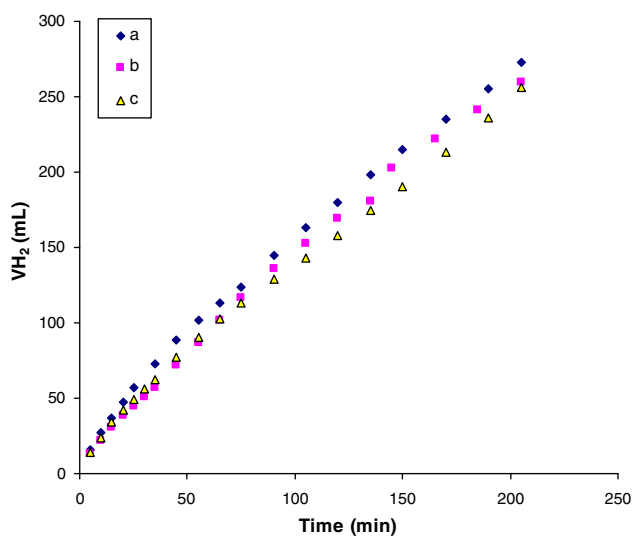


Fig. 3. Hydrogenation of nitrobenzene as catalysts Pd(II) complexes at 45 °C in DMF solution. (a = $[\text{Pd}(\text{L}_1)(\mu\text{-OAc})]_2$, b = $[\text{Pd}(\text{L}_2)(\mu\text{-OAc})]_2$, c = $[\text{Pd}(\text{L}_3)_2]$).

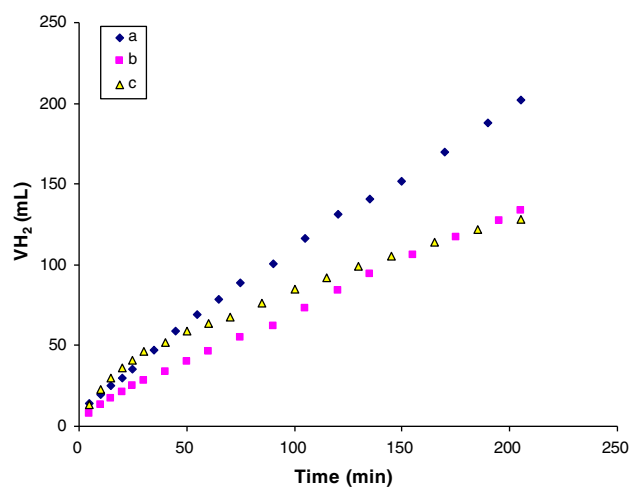


Fig. 4. Hydrogenation of nitrobenzene as catalysts Pd(II) complexes + NaBH_4 at 25 °C in DMF solution. (a = $[\text{Pd}(\text{L}_1)(\mu\text{-OAc})]_2$, b = $[\text{Pd}(\text{L}_2)(\mu\text{-OAc})]_2$, c = $[\text{Pd}(\text{L}_3)_2]$).

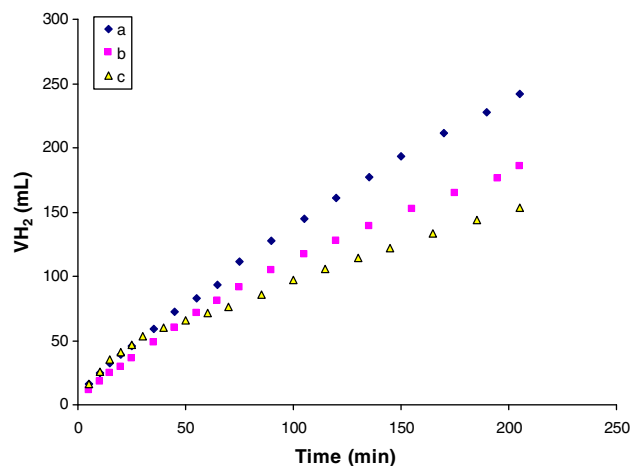


Fig. 5. Hydrogenation of nitrobenzene as catalysts Pd(II) complexes + NaBH_4 at 45 °C in DMF solution. (a = $[\text{Pd}(\text{L}_1)(\mu\text{-OAc})]_2$, b = $[\text{Pd}(\text{L}_2)(\mu\text{-OAc})]_2$, c = $[\text{Pd}(\text{L}_3)_2]$).

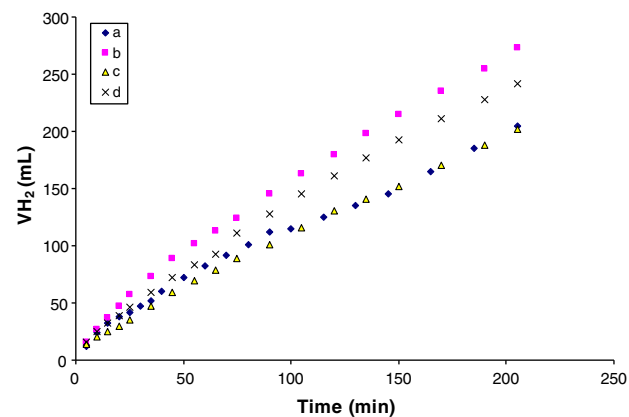


Fig. 6. Hydrogenation of nitrobenzene as $[\text{Pd}(\text{L}_3)_2]$ catalysts at 25 and 45 °C in DMF solution. (a = nitrobenzene (25 °C), b = nitrobenzene (45 °C), c = nitrobenzene + NaBH_4 (25 °C) and d = nitrobenzene + NaBH_4 (45 °C).

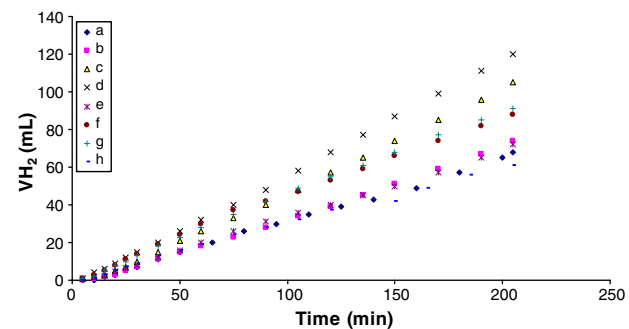
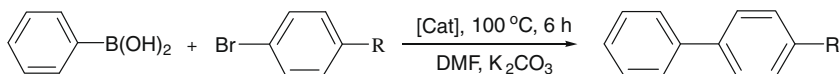


Fig. 7. Hydrogenation of cyclohexene as $[\text{Pd}(\text{L}_1)(\mu\text{-OAc})]_2$ and $[\text{Pd}(\text{L}_3)_2]$ catalysts at 25 and 45 °C in DMF solution. (a = 25 °C, b = 45 °C, c = NaBH_4 + 25 °C and d = NaBH_4 + 45 °C for $[\text{Pd}(\text{L}_1)(\mu\text{-OAc})]_2$ and (e = 25 °C, f = 45 °C, g = NaBH_4 + 25 °C and h = NaBH_4 + 45 °C for $[\text{Pd}(\text{L}_3)_2]$).

is obtained. We initially tested the catalytic activity of the Pd(II) metal complexes for the coupling of different aryl bromides with phenylboronic acid and the control experiments showed that the coupling reaction did not occur in the absence of the catalyst. Under these conditions, different aryl bromides react cleanly with phenylboronic acid in good yields (Table 3). The palladium-catalyzed reaction of aryl halides with arylboronic acids (the Suzuki



Scheme 5. The Suzuki–Miyaura coupling of different aryl bromides with phenylboronic acid

Table 3
The Suzuki–Miyaura coupling of different aryl bromides with phenylboronic acid.

Entry	[Cat] (complex)	R	Product	Yield (%) ^a	TON ^b	TOF (h ⁻¹) ^b
1	[Pd(L ₁)(μ-OAc)] ₂	H		93	93	16
2	[Pd(L ₂)(μ-OAc)] ₂	H		70	70	12
3	[Pd(L ₃) ₂]	H		88	88	15
4	[Pd(L ₁)(μ-OAc)] ₂	COCH ₃		82	82	14
5	[Pd(L ₂)(μ-OAc)] ₂	COCH ₃		93	93	16
6	[Pd(L ₃) ₂]	COCH ₃		97	97	16
7	[Pd(L ₁)(μ-OAc)] ₂	CHO		98	98	16
8	[Pd(L ₂)(μ-OAc)] ₂	CHO		97	97	16
9	[Pd(L ₃) ₂]	CHO		95	95	16
10	[Pd(L ₁)(μ-OAc)] ₂	NO ₂		88	88	15
11	[Pd(L ₂)(μ-OAc)] ₂	NO ₂		75	75	13
12	[Pd(L ₃) ₂]	NO ₂		95	95	16
13	[Pd(L ₁)(μ-OAc)] ₂	OMe		69	69	12
14	[Pd(L ₂)(μ-OAc)] ₂	OMe		59	59	10
15	[Pd(L ₃) ₂]	OMe		87	87	15

Reaction conditions: 1.0 mmol of *p*-R-C₆H₄Br; 1.5 mmol of phenylboronic acid; 2.0 mmol K₂CO₃; % 1.0 mmol Pd (Cat.) was used; DMF 3 mL; temperature 100 °C and at 6 h.

^a GC-yield using diethyleneglycol-di-*n*-butylether as internal standard

^b TON = mol product/mol cat. and TOF = (mol product/mol cat.) × h⁻¹.

coupling reaction) is the most common method for C–C bond formation [26,30,46]. The reactions are usually carried out homogeneously in the presence of a base under inert atmosphere. The reactivity of the aryl halide component decreases sharply in the order X = I > Br > Cl and electron-withdrawing substituents R are required for the chlorides to react [26,30,46–48]. The palladium-catalyzed cross-coupling reaction of phenylboronic acid with aryl bromides has been summarized in Table 3 and Scheme 5. The obtained results indicate that catalytic activities are correlated with the size of the Pd(II) metal complexes and location of bromo or methoxy substituent. From the results shown in Table 3, it is evident that the [Pd(L₁)(μ-OAc)]₂ complex is more efficient than the other complexes for the product one and three. The [Pd(L₃)₂] complex is more efficient than the other complexes for the product two, four and five.

3.3. Electrochemistry

The electrochemistry of the ligands (L₁H, L₂H and L₃H) and their palladium complexes [Pd(L₁)(μ-OAc)]₂, [Pd(L₂)(μ-OAc)]₂ and [Pd(L₃)₂] are studied by the cyclic voltammetry in the scan rates of 25–500 mV s⁻¹ in CH₂Cl₂ solution containing 0.1 M TBAP supporting electrolyte. The cyclic voltammograms (CVs) of the ligands are shown in Fig. 8 at 100 mV s⁻¹ scan rate. As seen, (L₂H) and (L₃H) ligands exhibited one irreversible reduction processes without corresponding anodic waves. (L₃H) ligand also showed second reduction wave with corresponding anodic wave as well as the first reduction process as observed for (L₂H) and (L₃H) ligands. The reduction processes of the ligands are based on the reduction of the azomethine nitrogen in the presence of the phenolic proton in the molecule. Mostly, the process results in the reductive coupling of the reduced species as previously observed for some Schiff bases such as Salen or its derivatives, indicating irreversible fashion of the processes [49–51]. However, the reduction process is probably assigned to the electro-deprotonated ligand anion at the platinum surface. The ligands (L₁H), (L₂H) and (L₃H) displayed the cathodic peak potentials at E_{pc} = –1.19, –1.65, and –1.78 V versus Ag/AgCl, respectively. The second reduction wave of (L₁H)

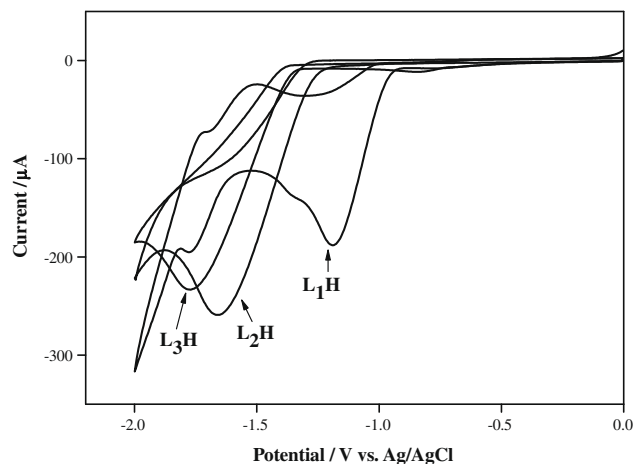


Fig. 8. Cyclic voltammograms (CVs) of the ligands in CH₂Cl₂ containing 0.1 M TBAP. Scan rate: 100 mV s⁻¹. Working electrode: a 1.6 mm diameter of glassy carbon electrode.

appeared at E_{pa} = –1.77 V. It is well known that the introduction of electron-donating or electron-withdrawing groups to the electroactive molecules is expected to lead to an increase or decrease of electron density in the molecule, thereby making the molecule easier to oxidise and harder to reduce or vice versa [52–56]. This effect was clearly demonstrated by the fact that the cathodic peak potential of (L₁H) was shifted towards more positive potentials compared to those of (L₂H) and (L₃H). It is strongly attributed to the electron-withdrawing bromo group substituted on the benzene ring. Therefore, the second reduction process for (L₁H) could be observed within the electrochemical scale studied. The cyclic voltammogram (CV) of [Pd(L₂)(μ-OAc)]₂ in the scan rate of 100 mV s⁻¹ is exhibited in Fig. 9. Where the inset figure represents CVs of the complex in the scan rates of 25–500 mV s⁻¹ between 0 and 1.2 V potential ranges. The data corresponding to the cyclic voltammograms (CVs) of the ligands and their complexes are also listed in Table 4. [Pd(L₂)(μ-OAc)]₂ and [Pd(L₃)₂] showed two oxidation

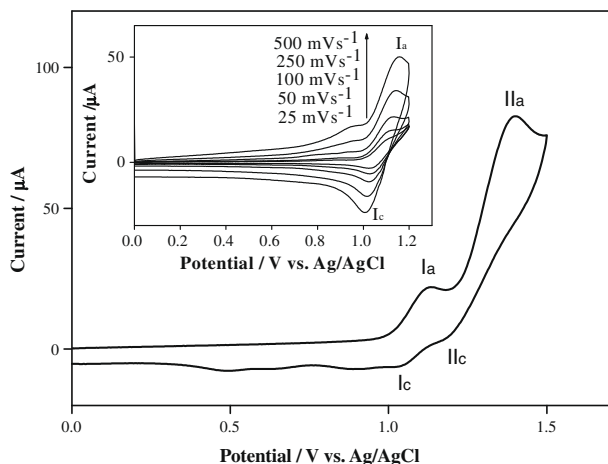


Fig. 9. Cyclic voltammogram (CV) of $[\text{Pd}(\text{L}_2)(\mu\text{-OAc})_2]$ in CH_2Cl_2 containing 0.1 M TBAP. Scan rate: 100 mV s^{-1} . The inset figure is represents CVs of the complex in the scan rates of $25\text{--}500 \text{ mV s}^{-1}$ between 0 and 1.2 V potential ranges. Working electrode: a 1.6 mm diameter of glassy carbon electrode.

Table 4

Voltammetric data for the ligands and their palladium complexes vs. Ag/AgCl (Fc/Fc⁺): values in parentheses vs. Fc/Fc⁺ in $\text{CH}_2\text{Cl}_2\text{-TBAP}$.

Complexes	L/L ⁻ E_{pc}^{a} (V)	L/L ⁺ $E_{1/2}^{\text{c}}$ (V)	Pd ²⁺ /Pd ⁴⁺ E_{pa}^{b} (V)	ΔE^{d} (V)
(L ₁ H)	-1.19 (-1.69)			
	-1.77 ^e (-2.27)			
(L ₂ H)	-1.65 (-2.15)			
(L ₃ H)	-1.78 (-2.28)			
$[\text{Pd}(\text{L}_1)(\mu\text{-OAc})_2]$	-1.23 (-1.73)			
$[\text{Pd}(\text{L}_2)(\mu\text{-OAc})_2]$		1.07 (0.57)	1.40 (0.90)	0.070
$[\text{Pd}(\text{L}_3)_2]$		1.08 (0.58)	1.39 (0.89)	0.060

^a E_{pc} : cathodic peak for reduction and oxidation for irreversible processes.

^b E_{pa} : anodic potentials for reduction and oxidation for irreversible processes.

^c $E_{1/2} = E_{\text{pc}} + E_{\text{pa}}/2$.

^d $\Delta E_{\text{p}} = E_{\text{pc}} - E_{\text{pa}}$ at 100 mV s^{-1} scan rate for the first reversible oxidation processes.

^e -1.77 = the second reduction potential of (L₁H).

processes in the scan rate of 100 mV s^{-1} probably based on the ligand and metal center. The anodic (I_{a}) – cathodic (I_{c}) peak separations (ΔE) for the first oxidations of $[\text{Pd}(\text{L}_2)(\mu\text{-OAc})_2]$ and $[\text{Pd}(\text{L}_3)_2]$ are 0.070 and 0.060 V (scan rate: 50 mV s^{-1}), respectively which assign to the reversible processes. The half-wave potentials ($E_{1/2}$) of these reversible redox couples were calculated as the average of the cathodic (I_{c}) and anodic (I_{a}) peak potentials of the processes. The $E_{1/2}$ of the reduction processes of $[\text{Pd}(\text{L}_2)(\mu\text{-OAc})_2]$ and $[\text{Pd}(\text{L}_3)_2]$ are 1.07, 1.08 V versus Ag/AgCl, respectively. The second oxidation processes of the $[\text{Pd}(\text{L}_2)(\mu\text{-OAc})_2]$ and $[\text{Pd}(\text{L}_3)_2]$ exhibiting a large anodic (I_{a}) – cathodic (I_{c}) peak separation have irreversible fashion. Their anodic peak potentials (E_{pa}) was observed at 1.40 and 1.39 V. $[\text{Pd}(\text{L}_3)_2]$ also showed one irreversible reduction process at $E_{\text{pc}} = -1.49 \text{ V}$ but not for $[\text{Pd}(\text{L}_2)(\mu\text{-OAc})_2]$ in the same experimental conditions, probably due to different structures of the complexes. $[\text{Pd}(\text{L}_1)(\mu\text{-OAc})_2]$ showed only one irreversible reduction wave at $E_{\text{pc}} = -1.23 \text{ V}$ but not any oxidation couples. The expected oxidation waves of $[\text{Pd}(\text{L}_1)(\mu\text{-OAc})_2]$ probably shifted toward out of the scale due to the presence of electron-withdrawing bromo groups on $[\text{Pd}(\text{L}_1)(\mu\text{-OAc})_2]$. It is evaluated from the inset figure (Fig. 9.) that the first oxidation process of $[\text{Pd}(\text{L}_2)(\mu\text{-OAc})_2]$ is diffusion controlled with the anodic current function ($I_{\text{pa}}/v^{1/2}$) independent of the scan rate (v) over the scan range $25\text{--}500 \text{ mV s}^{-1}$ [52–56].

4. Conclusions

In this study, the five salicylaldimine ligands (L₁H, L₂H, L₃H, L₄H and L₅H) and their orthopalladation dinuclear $[\text{Pd}(\text{L}_1)(\mu\text{-OAc})_2]$, $[\text{Pd}(\text{L}_2)(\mu\text{-OAc})_2]$ and mononuclear $[\text{Pd}(\text{L}_3)_2]$ metal complexes were synthesized and characterized by elemental analyses, FT-IR, UV-Vis, ¹H and ¹³C NMR spectra, molar conductivity, as well as by electrochemical techniques. The L₁H and L₂H are coordinated through the imine nitrogen and aromatic *ortho* carbon atoms, whereas the ligand L₃H is coordinated through the imine nitrogen and phenolic oxygens atoms. The catalytic studies showed that the introduction of different groups on the salicyl rings of the molecules increased the catalytic activity towards hydrogenation of nitrobenzene and cyclohexene in DMF at 25 and 45 °C. The electron-donating/withdrawing and other functional groups probably increases the electron density on the Pd atom, which is subjected to electrophilic attack by a nitro group of nitrobenzene and a double bond of cyclohexene. Also, the obtained Suzuki–Miyaura coupling reaction results indicate that catalytic activities are correlated to the size of the Pd(II) complexes and to the position of the bromo or methoxy substituents.

Acknowledgements

This work has been supported, in part, by the Research Fund of Harran University (Sanliurfa, Turkey).

References

- [1] I. Omae, Organometallic-Coordination Compounds, Elsevier, Amsterdam, New York, 1986.
- [2] A.D. Ryabov, Chem. Rev. 90 (1990) 403.
- [3] M. Pfeffer, Recl. Trav. Chim. Pays-Bas 109 (1990) 567.
- [4] J.M. Vila, M.T. Pereira, J.M. Ortigueira, M. Grana, D. Lata, A. Suarez, J.J. Fernandez, A. Fernandez, M. Lopez-Torres, H. Adams, J. Chem. Soc., Dalton Trans. (1999) 4193.
- [5] M. Pfeffer, J.P. Sutter, M.A. Rottvel, A. de Cian, J. Fischer, Tetrahedron 48 (1992) 2440.
- [6] A. Bose, C.H. Saha, J. Mol. Catal. 49 (1989) 271.
- [7] J.M. Vila, M.T. Pereira, J.M. Ortigueira, J.J. Fernandez, A. Fernandez, M. Lopez-Torres, H. Adams, Organometallics 18 (1999) 5484.
- [8] J.J. Fernandez, A. Fernandez, D.V. Garcia, M. Lopez-Torres, A. Suarez, N.G. Blanco, J.M. Vila, Eur. J. Inorg. Chem. (2007) 5408.
- [9] J. Albert, R.M. Ceder, M. Gomez, J. Granell, J. Sales, Organometallics 11 (1992) 1536.
- [10] D.J. Cardenas, A.M. Echavarren, A. Vegas, Organometallics 13 (1994) 882.
- [11] J.W. Canary, B.C. Gibb, in: K.D. Karlin (Ed.), Progress in Inorganic Chemistry, vol. 45, Wiley, New York, 1997, p. 1.
- [12] C. Lopez, A. Caubet, S. Perez, X. Solans, M. Font-Bardia, J. Organomet. Chem. 681 (2003) 82.
- [13] V.T. Kasumov, E. Tas, F. Köksal, S.O. Yaman, Polyhedron 24 (2005) 319.
- [14] E. Steiner, F.A.L. L'Eplattenier, Helv. Chim. Acta 61 (1978) 2264.
- [15] A.K. Mahapatra, D. Bandyopadhyay, P. Bandyopadhyay, A. Chakravorty, Inorg. Chem. 25 (1986) 2214.
- [16] V. Arun, N. Sridevi, P.P. Robinson, S. Manju, K.K.M. Yusuff, J. Mol. Catal. A: Chem. 304 (1–2) (2009) 191.
- [17] J. March, Advanced Organic Chemistry: Reactions, Mechanisms and Structure, fourth ed., Wiley-Interscience, New York, 1992, p. 780.
- [18] A. Andriollo, A. Bolivar, F.A. Lopez, D.E. Pdez, Inorg. Chim. Acta 238 (1995) 187.
- [19] C. Dagueuet, R. Scopelliti, D.J. Dyson, Organometallics 23 (2004) 4849.
- [20] D.G. Holah, A.N. Hughes, B.C. Hui, C.T. Kan, J. Catal. 48 (1977) 340.
- [21] I.M. Angulo, E. Bouwman, J. Mol. Catal. A: Chem. 175 (2001) 65.
- [22] C.R. Landis, J. Halpren, Organometallics 2 (1983) 840.
- [23] J.A. Widegren, M.A. Bennett, R.G. Fink, J. Am. Chem. Soc. 125 (34) (2003) 10301.
- [24] S. Burling, Adv. Synth. Catal. 347 (2005) 591.
- [25] D.A. Alonso, C. Najera, M.C. Pacheco, Org. Lett. 2 (13) (2000) 1823.
- [26] S.P. Stanforth, Tetrahedron 54 (1998) 263.
- [27] J. Tsuji, Palladium Reagents and Catalysts: Innovations in Organic Synthesis, Wiley, Chichester, 1995.
- [28] L. Botella, C. Najera, Angew. Chem., Int. Ed. 41 (2002) 1.
- [29] A. Suzuki, J. Organomet. Chem. 576 (1999) 147.
- [30] N. Miyaura, A. Suzuki, Chem. Rev. 95 (1995) 2457.
- [31] S. Haber, H.J. Kleiner (Hoescht AG), DE 19527118, Chem. Abstr. 126 (1997) 185894.
- [32] O.N. Kaddin, J. An, H. Han, Y.G. Galyametdinov, Eur. J. Inorg. Chem. 10 (2008) 1682.

- [33] P. Bandyopadhyay, P.K. Mascharak, A. Chakravorty, *J. Chem. Soc., Dalton Trans.* (1982) 675.
- [34] E. Tas, A. Kilic, M. Durgun, I. Yilmaz, I. Ozdemir, N. Gurbuz, *J. Organomet. Chem.* 694 (2009) 446.
- [35] J.M. Vila, M. Gayoso, M.T. Pereira, M. Lopez-Torres, J.J. Fernandez, A. Fernandez, J.M. Ortigueira, *J. Organomet. Chem.* 506 (1996) 165.
- [36] E. Tas, A. Kilic, N. Konak, I. Yilmaz, *Polyhedron* 27 (2008) 1024.
- [37] A. Kilic, E. Tas, B. Deveci, I. Yilmaz, *Polyhedron* 26 (2007) 4009.
- [38] B. Tejjido, A. Fernandez, M. Lopez-Torres, S. Castro-Luiz, A. Suarez, J.M. Ortigueira, J.M. Vila, J.J. Fernandez, *J. Organomet. Chem.* 598 (2000) 71.
- [39] L. Sacconi, M. Ciampolini, F. Maffio, F.P. Cavasino, *J. Am. Chem. Soc.* 84 (1962) 3245.
- [40] R.L. Carlin, *Transition Met. Chem.*, vol. 1, Marcel Dekker, New York, 1965.
- [41] C. Fraser, B. Bosnich, *Inorg. Chem.* 33 (1994) 338.
- [42] A.B.P. Lever, *Inorganic Electronic Spectroscopy*, Elsevier, Amsterdam, 1984.
- [43] E. Tas, I.H. Onal, I. Yilmaz, A. Kilic, M. Durgun, *J. Mol. Struct.* 927 (2009) 69.
- [44] J.A. Widegren, R.G. Finke, *J. Mol. Catal. A: Chem.* 191 (2003) 187.
- [45] C.M. Hagen, J.A. Widegren, P.M. Maitlis, R.G. Finke, *J. Am. Chem. Soc.* 127 (2005) 4423.
- [46] G.T. Crisp, *Chem. Soc. Rev.* 27 (1998) 427.
- [47] A.F. Littke, G.F. Fu, *Angew. Chem., Int. Ed. Engl.* 41 (2002) 4176.
- [48] R.B. Bedford, S.L. Hazewood, M.E. Limmeat, *Chem. Commun.* (2002) 2610.
- [49] A.A. Isse, A. Gennaro, E. Vianello, *Electrochim. Acta* 42 (1997) 2065.
- [50] T. Shono, N. Kise, E. Shirakawa, H. Matsumoto, E. Okazaki, *J. Org. Chem.* 56 (1991) 3063.
- [51] N. Kise, H. Oike, E. Okazaki, M. Yoshimoto, T. Shono, *J. Org. Chem.* 60 (1995) 3980.
- [52] I. Yilmaz, A.G. Gurek, V. Ahsen, *Polyhedron* 24 (2005) 791.
- [53] I. Yilmaz, M. Kocak, *Polyhedron* 23 (2004) 1279.
- [54] K.M. Kadish, T. Nakanishi, V. Ahsen, I. Yilmaz, *J. Phys. Chem. B* 105 (2001) 9817.
- [55] E. Tas, M. Ulusoy, M. Guler, I. Yilmaz, *Transition Met. Chem.* 29 (2004) 180.
- [56] A. Kilic, E. Tas, B. Gumgum, I. Yilmaz, *Transition Met. Chem.* 31 (2006) 645.